TCDD vs TCDF

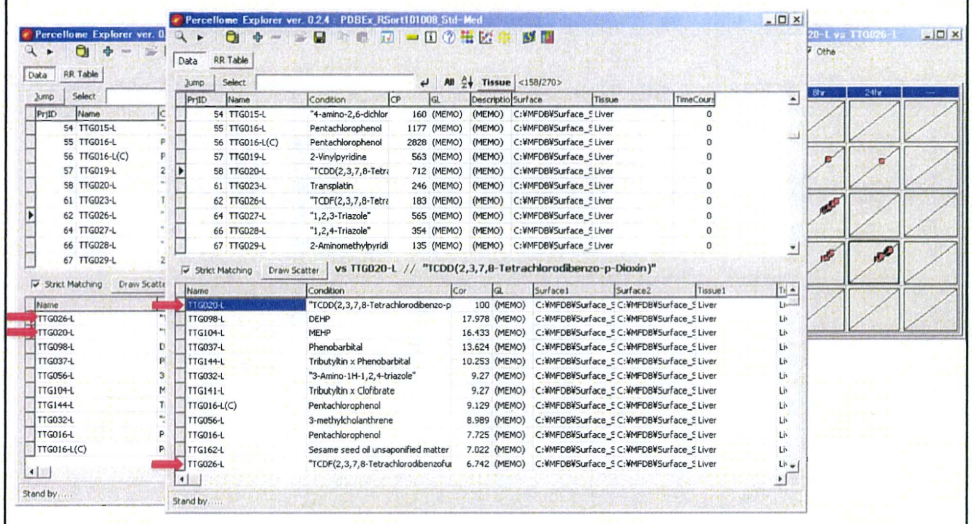

17

DEHP vs MEHP

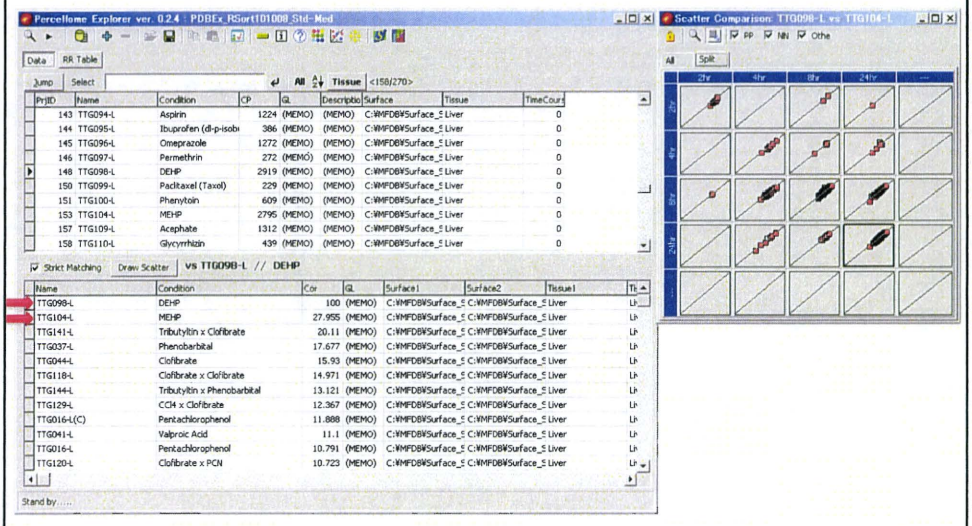

18

CoQ10(Single) vs CoQ10(Repeat14days)

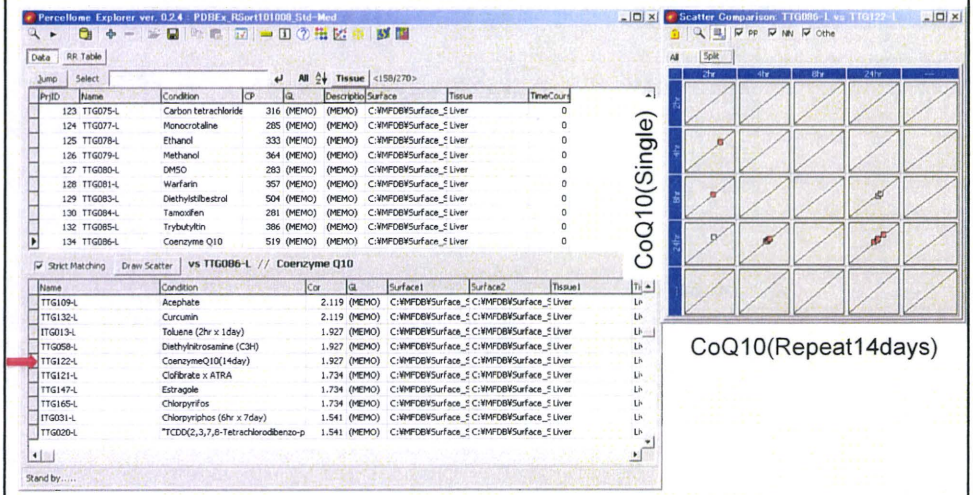

19

Diethylnitrosoamine: C57Bl/6 vs C3H

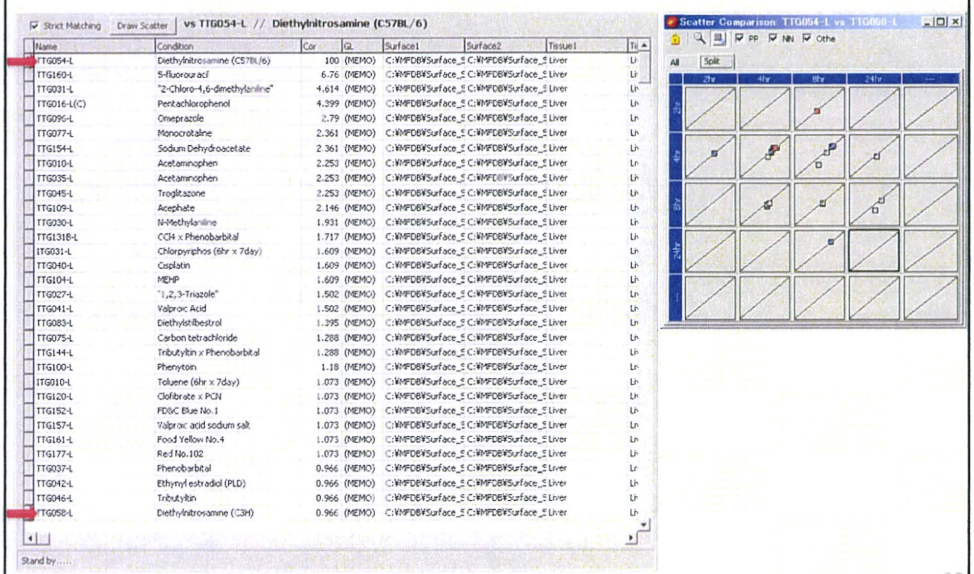

20

Valproic Acid関連プロジェクトでの比較

Name	Condition	Cor
TTG157-L	Valproic acid sodium salt	100.00
TTG041-L	Valproic Acid	16.43
TTG151-L	Valproic acid sodium salt x Valproic acid sodium salt	16.27
TTG098-L	DEHP	12.03
TTG104-L	MEHP	10.59
TTG037-L	Phenobarbital	9.72
TTG016-L(C)	Pentachlorophenol	9.52
TTG154-L	Sodium Dehydroacetate	9.52
TTG141-L	Tributyltin x Clofibrate	8.96
TTG044-L	Clofibrate	7.93
TTG118-L	Clofibrate x Clofibrate	6.96
TTG129-L	CCl4 x Clofibrate	6.86
ITG012-L	Formaldehyde (2hr x 1day)	5.22
TTG073-L	Toluene	5.02
TTG149-L	Valproic acid sodium salt x Aspirin	5.02
TTG144-L	Tributyltin x Phenobarbital	4.30
TTG046-L	Tributyltin	4.25
TTG109-L	Acephate	4.25
TTG062-L(C)	Dexamethasone	3.94
TTG087-L	Pyriproxyfen	3.89
TTG032-L	3-Amino-1H-1,2,4-triazole	3.84
TTG182-L	Sesame seed oil unsaponified matter	3.74
TTG136-L	Phytol	3.48
TTG053-L	Ethynyl estradiol (PLD)	3.28
TTG016-L	Pentachlorophenol	3.22
ITG012-L	Toluene (2hr x 1day)	3.17
TTG094-L	Aspirin	3.17
TTG120-L	Clofibrate x PCN	3.07
TTG031-L	2-Chloro-4,6-dimethylaniline	3.02
TTG185-L	Chlorpyrifos	2.87
TTG059-L	Caffeine	2.76
TTG096-L	Omeprazole	2.41
TTG086-L	Methoprene	2.35
TTG131B-L	CCl4 x Phenobarbital	2.35
TTG160-L	5-fluorouracil	2.30
TTG019-L	2-Vinylpyridine	2.15
TTG090-L	Pregnenolone Carbonitrile	2.05
TTG121-L	Clofibrate x ATRA	2.05
ITG025-L	Tetradecane (6hr x 7day)	1.95
TTG074-L	Bromobenzene	1.89
TTG122-L	Coenzyme Q10(14day)	1.89
TTG147-L	Estragole	1.89
TTG056-L	3-methylcholanthrene	1.84
TTG095-L	Ibuprofen (dl-p-isobutylhydratropic acid)	1.84
TTG100-L	Phenytoin	1.79
ITGC001-L	Formalin (6hr x 7day)	1.74
TTG166-L	Carbaryl	1.74
TTG020-L	TCDD(2,3,7,8-Tetrachlorodibenzo-p-Dioxin)	1.69
TTG051-L	9-cis retinoic acid	1.69
TTG150-L	Valproic acid sodium salt x Thalidomide	1.64

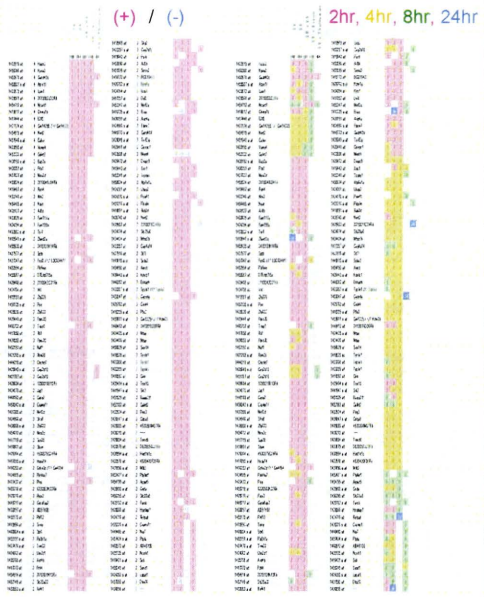

21

Valproic Acid関連プロジェクトでの比較

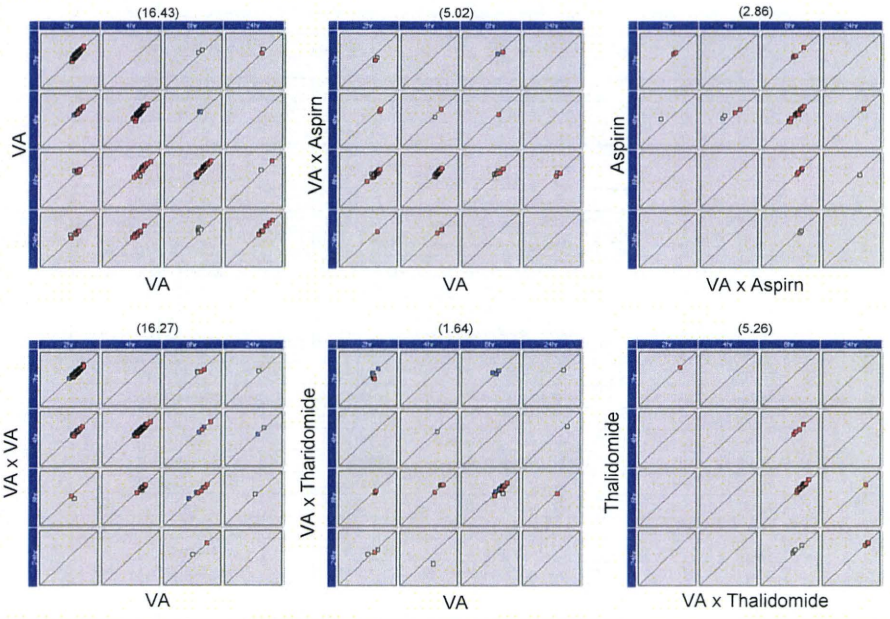

22

類似反応の例

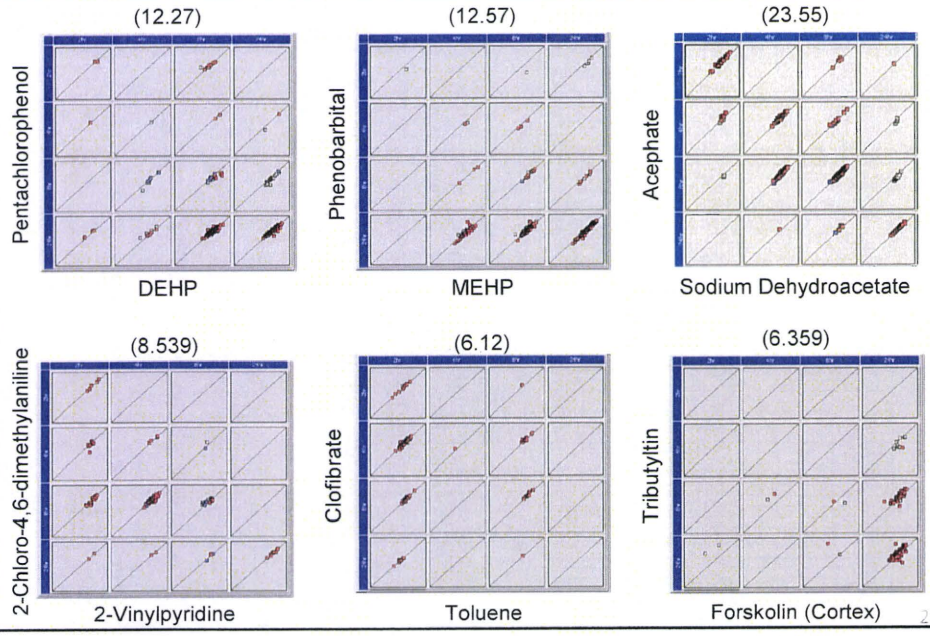

23

類似度Top1～25

Ord	Cor.	Prj #1		Prj #2		
1	34.257	TTG144-L	TTG2: A)Tributyltin, B)Phenobarbital	TTG037-L	Phenobarbital sodium	
2	31.238	TTG120-L	TTG2: A)Clofibrate, B)PCN	TTG098-L	DEHP	
3	30.852	TTG129-L	TTG2: A)CCl4, B)Clofibrate	TTG141-L	TTG2: A)Tributyltin, B)Clofibrate	
4	29.195	TTG104-L	MEHP	TTG098-L	DEHP	
5	28.067	TTG118-L	TTG2: A)Clofibrate, B)Clofibrate	TTG098-L	DEHP	
6	27.955	TTG098-L	DEHP	TTG104-L	MEHP	
7	27.886	TTG019-L	2-Vinylpyridine	TTG154-L	Sodium Dehydroacetate	*
8	27.374	TTG062-L(C)	Dexamethasone	TTG154-L	Sodium Dehydroacetate	
9	27.232	TTG118-L	TTG2: A)Clofibrate, B)Clofibrate	TTG141-L	TTG2: A)Tributyltin, B)Clofibrate	
10	27.221	TTG144-L	TTG2: A)Tributyltin, B)Phenobarbital	TTG098-L	DEHP	
11	26.821	TTG019-L	2-Vinylpyridine	TTG109-L	Acephate	*
12	26.777	TTG165-L	Chlorpyrifos	TTG154-L	Sodium Dehydroacetate	
13	26.763	TTG016-L	Pentachlorophenol	TTG098-L	DEHP	
14	26.552	TTG032-L	3-Amino-1H-1,2,4-triazole	TTG098-L	DEHP	
15	26.465	TTG019-L	2-Vinylpyridine	TTG104-L	MEHP	
16	26.346	TTG044-L	Clofibrate	TTG098-L	DEHP	
17	26.344	TTG030-L	N-Methylaniline	TTG154-L	Sodium Dehydroacetate	
18	26.230	TTG026-L	TCDF	TTG020-L	TCDD	*
19	25.985	TTG141-L	TTG2: A)Tributyltin, B)Clofibrate	TTG098-L	DEHP	
20	25.841	TTG129-L	TTG2: A)CCl4, B)Clofibrate	TTG098-L	DEHP	
21	25.573	TTG016-L	Pentachlorophenol	TTG016-L(C)	Pentachlorophenol	*
22	25.496	TTG162-L	Sesame seed oil unsaponified matter	TTG098-L	DEHP	
23	25.400	TTG019-L	2-Vinylpyridine	TTG098-L	DEHP	
24	25.393	TTG109-CX	Acephate	TTG109-HC	Acephate	*
25	24.971	TTG131B-L	TTG2: A)CCl4, B)Phenobarbital	TTG144-L	TTG2: A)Tributyltin, B)Phenobarbital	

24

類似度Top26～50

Ord	Cor.	Prj #1		Prj #2		
26	24.759	TTG044-L	Clofibrate	TTG141-L	TTG2: A)Tributyltin, B)Clofibrate	
27	24.696	TTG129-L	TTG2: A)CCl4, B)Clofibrate	TTG104-L	MEHP	
28	24.609	TTG090-L	5-Pregnen-3beta-ol-20-one-16alpha-carbonitrile	TTG098-L	DEHP	
29	24.553	TTG129-L	TTG2: A)CCl4, B)Clofibrate	TTG118-L	TTG2: A)Clofibrate, B)Clofibrate	
30	24.551	TTG162-L	Sesame seed oil unsaponified matter	TTG037-L	Phenobarbital sodium	
31	24.338	TTG129-L	TTG2: A)CCl4, B)Clofibrate	TTG044-L	Clofibrate	
32	24.331	TTG151-L	TTG2: A)Valproic acid sodium salt, B)Valproic acid sodium salt	TTG157-L	Valproic acid sodium salt	*
33	24.165	TTG034-L	4-Ethylnitrobenzene	TTG154-L	Sodium Dehydroacetate	
34	23.845	TTG157-H	Valproic acid sodium salt	TTG157-G	Valproic acid sodium salt	
35	23.735	TTG168-L	Mastic	TTG098-L	DEHP	
36	23.699	TTG118-L	TTG2: A)Clofibrate, B)Clofibrate	TTG044-L	Clofibrate	
37	23.552	TTG109-L	Acephate	TTG154-L	Sodium Dehydroacetate	*
38	23.443	TTG119-G	TTG2: CCl4	ITG017-G	Xylene(2hr x 1day)	
39	23.343	TTG044-L	Clofibrate	TTG104-L	MEHP	
40	23.316	TTG141-L	TTG2: A)Tributyltin, B)Clofibrate	TTG095-L	Ibuprofen (dl-p-isobutylhydratropic acid)	
41	23.126	059-L	Caffeine	154-L	Sodium Dehydroacetate	
42	23.118	030-L	N-Methylaniline	109-L	Acephate	
43	23.057	118-L	TTG2: A)Clofibrate, B)Clofibrate	104-L	MEHP	
44	22.879	034-L	4-Ethylnitrobenzene	109-L	Acephate	*
45	22.854	120-L	TTG2: A)Clofibrate, B)PCN	037-L	Phenobarbital sodium	
46	22.380	019-L	2-Vinylpyridine	041-K	Valproic acid sodium salt	
47	22.175	016-L	Pentachlorophenol	104-L	MEHP	*
48	22.096	162-L	Sesame seed oil unsaponified matter	144-L	TTG2: A)Tributyltin, B)Phenobarbital	
49	22.030	118-L	TTG2: A)Clofibrate, B)Clofibrate	129-L	TTG2: A)CCl4, B)Clofibrate	
50	21.813	157-CX	Valproic acid sodium salt	157-HC	Valproic acid sodium salt	*

25

要素数1000以上のプロジェクト(肝のみ)

Name	Condition	CP
ITG012-L	Formaldehyde (2hr x 1day)	3884
TTG037-L	Phenobarbital	3221
TTG098-L	DEHP	2919
TTG016-L(C)	Pentachlorophenol	2828
TTG104-L	MEHP	2795
TTG154-L	Sodium Dehydroacetate	2552
TTG041-L	Valproic Acid	2402
ITGC001-L	Formalin (6hr x 7day)	2371
TTG141-L	Tributyltin x Clofibrate	2259
TTG157-L	Valproic acid sodium salt	1954
TTG053-L	Ethynyl estradiol (PLD)	1872
TTG073-L	Toluene	1803
TTG044-L	Clofibrate	1765
TTG122-L	CoenzymeQ10(14day)	1613
TTG087-L	Pyriproxyfen	1597
TTG118-L	Clofibrate x Clofibrate	1557
TTG180-L	5-fluorouracil	1535
TTG046-L	Tributyltin	1494
TTG144-L	Tributyltin x Phenobarbital	1407
TTG129-L	CCl4 x Clofibrate	1397
TTG109-L	Acephate	1312
TTG151-L	Valproic acid sodium salt x Valproic acid sodium salt	1307
TTG096-L	Omeprazole	1272
TTG136-L	Phytol	1261
TTG094-L	Aspirin	1224
TTG031-L	"2-Chloro-4,6-dimethylaniline"	1218
TTG016-L	Pentachlorophenol	1177
TTG032-L	"3-Amino-1H-1,2,4-triazole"	1160
TTG149-L	Valproic acid sodium salt x Aspirin	1143
TTG089-L	Rifampicin	1082
TTG182-L	Sesame seed oil unsaponified matter	1059
TTG132-L	Curcumin	1009
TTG120-L	Clofibrate x PCN	1002

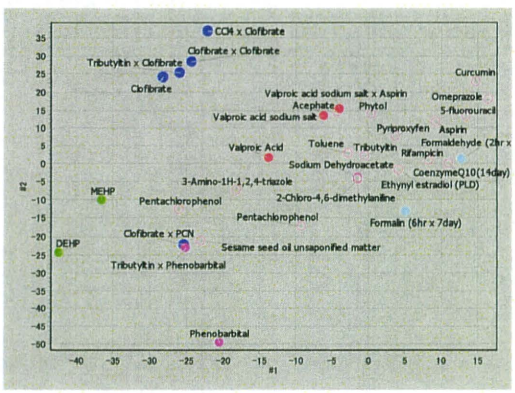

26

高頻度発現遺伝子の多要素プロジェクトでの発現状況

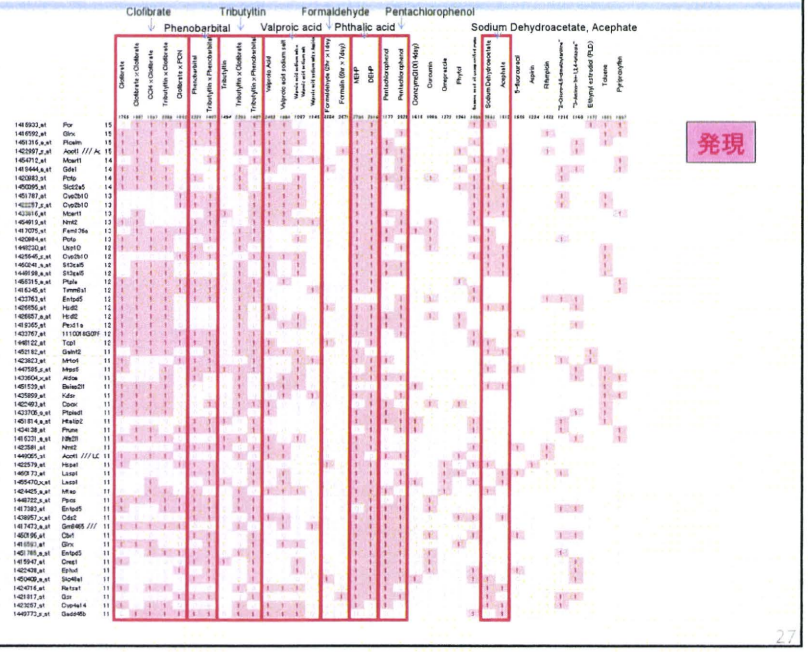

27

高頻度発現遺伝子の多要素プロジェクトでの発現状況

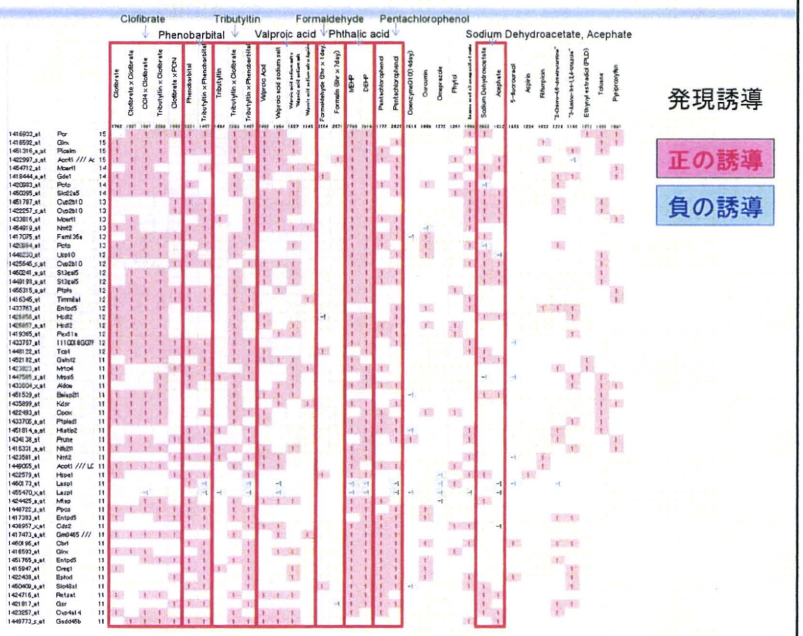

28

高頻度発現遺伝子の多要素プロジェクトでの発現状況

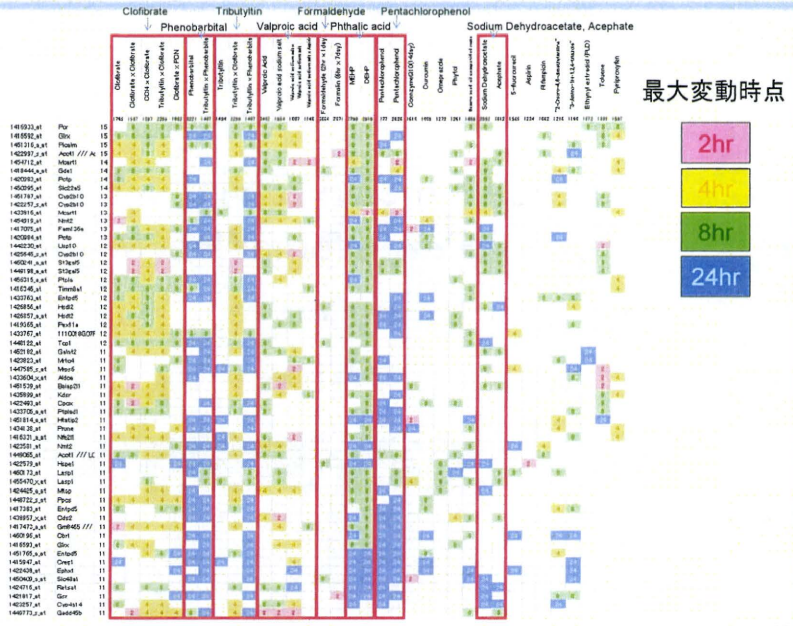

29

類似反応解析を中心とした研究・試験システム

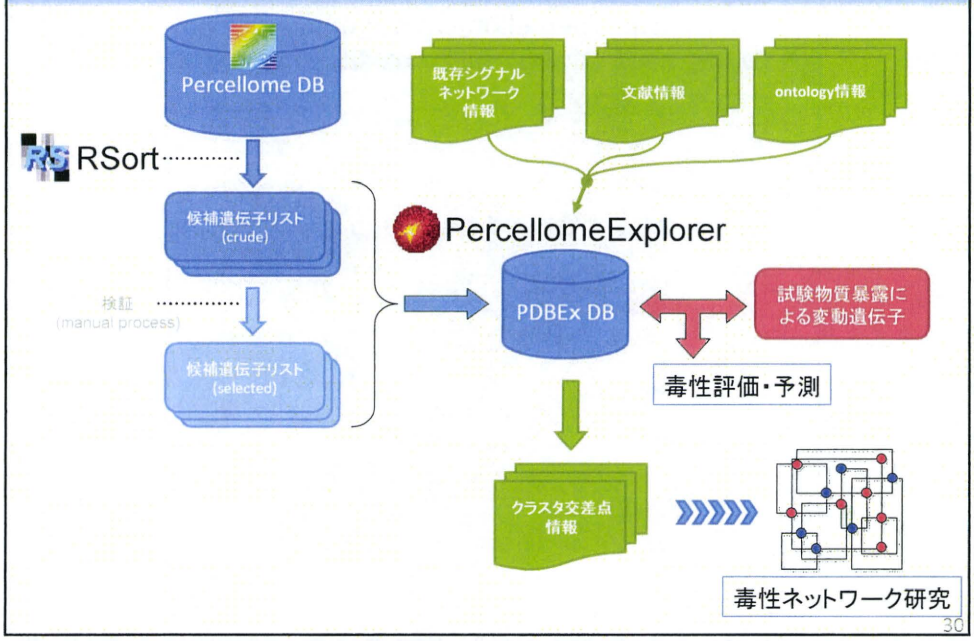

30

PercellomeDB公開サービス (PercellomeWeb)

<New Version>

Beta test中

http://percellome.nihs.go.jp

31

PercellomeWeb

http://percellome.nihs.go.jp

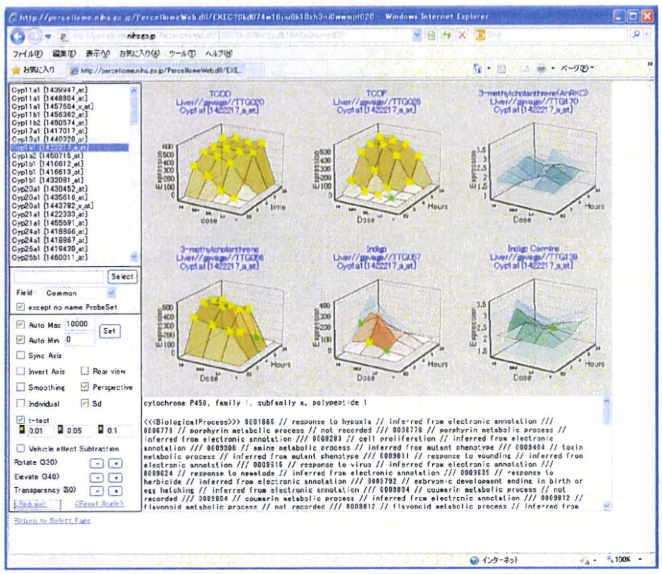

32

PercellomeWeb～MiniSurface

http://percellome.nihs.go.jp

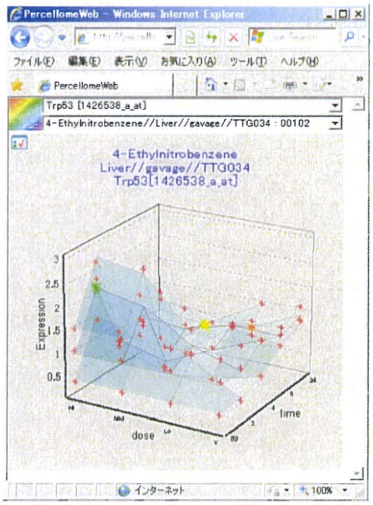

- 外部連携用の簡易ユーザーインターフェイス
- Login不要（使い捨ての認証コード用いる）
- 他のツールと異なり、化学物質を次々に切り替えて、特定の遺伝子発現パターンを閲覧することが出来る。

33

H23年度の方針

毒性ネットワーク解析・描画に加え、

- PercellomeWeb（データベース公開用Webアプリケーション）の機能拡充、特にGARUDA連携
- 時系列解析技術の再開発（DfSurface,SSなど）
- RSortの最適化
- TGPデータのインポート（Surfaceグラフ化）

34

別添５

Ⅲ．研究成果の刊行に関する一覧表

発表者氏名	論文タイトル名	発表誌名	巻名	ページ	出版年
Atsushi Baba, Fumiaki Ohtake, Yosuke Okuno, Kenichi Yokota, Maiko Okada, Yuuki Imai, Min Ni, Clifford A Meyer, Katsuhide Igarashi, Jun Kanno, Myles Brown, and Shigeaki Kato	Signal-sensing activation of a histone lysine demethylase complex	Nature Cell Biology			accept-ed
Arase S, Ishii K, Igarashi K, Aisaki K, Yoshio Y, Matsushima A, Shimohigashi Y, Arima K, Kanno J, Sugimura Y.	Endocrine Disrupter Bisphenol A Increases In Situ Estrogen Production in the Mouse Urogenital Sinus.	Biol Reprod.	84 (4)	734 - 742	2011
Yoshida T, Sekine T, Aisaki K, Mikami T, Kanno J, Okayasu I.	CITED2 is activated in ulcerative colitis and induces p53-dependent apoptosis in response to butyric acid.	J Gastroenterol	46 (3)	339 - 349	2011
Oginuma M, Takahashi Y, Kitajima S, Kiso M, Kanno J, Kimura A and Saga Y	The oscillation of Notch activation, but not its boundary, is required for somite border formation and rostral-caudal patterning within a somite.	Development	137	1515 - 1522	2011
菅野 純	Percellome トキシコゲノミクスの進捗	医学のあゆみ	236 (12)	1125 - 1126	2011
Matsuoka, Y.; Ghosh, S.; Kikuchi, N.; Kitano, H.	Payao - A Community Platform for Pathway Model Curation.	Bio-informatics	26 (10)	1381 - 1383	2010
Kitano, H.	Grand challenges in systems physiology. Frontiers in Systems Physiology.	Frontiers in Systems Physiology.	1 (3)	doi: 10.3389/fphys.2010.00003	2010
Kitano, H.	Violations of robustness trade-offs.	Molecular Systems Biology.	6 (384)	doi: 10.1038/msb.2010.40	2010
Shiraishi, T.; Matsuyama, S.; Kitano, H.	Large-Scale Analysis of Network Bistability for Human Cancers.	PLoS Computational Biology.	6 (7)	e1000851. doi:10.1371/journal.pcbi.1000851	2010
Ghosh, S., Matsuoka, Y., Kitano, H.	Connecting the dots: role of standardization and technology sharing in biological simulation.	Drug Discovery Today	15 23/24	1024 - 1031	2010

Ⅳ. 研究成果の刊行物・別刷り

BIOLOGY OF REPRODUCTION 84, 734–742 (2011)
Published online before print 1 December 2010.
DOI 10.1095/biolreprod.110.087502

Endocrine Disrupter Bisphenol A Increases In Situ Estrogen Production in the Mouse Urogenital Sinus[1]

Shigeki Arase,[3,5] Kenichiro Ishii,[3,4,5] Katsuhide Igarashi,[6] Kenichi Aisaki,[6] Yuko Yoshio,[5] Ayami Matsushima,[7] Yasuyuki Shimohigashi,[7] Kiminobu Arima,[5] Jun Kanno,[6] and Yoshiki Sugimura[2,5]

Department of Nephro-Urologic Surgery and Andrology,[5] Mie University Graduate School of Medicine, Mie, Japan
Division of Cellular & Molecular Toxicology,[6] National Institute of Health Sciences, Tokyo, Japan
Laboratory of Structure-Function Biochemistry,[7] Department of Chemistry, Faculty of Sciences, Kyushu University, Fukuoka, Japan

ABSTRACT

The balance between androgens and estrogens is very important in the development of the prostate, and even small changes in estrogen levels, including those of estrogen-mimicking chemicals, can lead to serious changes. Bisphenol A (BPA), an endocrine-disrupting chemical, is a well-known, ubiquitous, estrogenic chemical. To investigate the effects of fetal exposure to low-dose BPA on the development of the prostate, we examined alterations of the in situ sex steroid hormonal environment in the mouse urogenital sinus (UGS). In the BPA-treated UGS, estradiol (E_2) levels and CYP19A1 (cytochrome P450 aromatase) activity were significantly increased compared with those of the untreated and diethylstilbestrol (DES)-treated UGS. The mRNAs of steroidogenic enzymes, *Cyp19a1* and *Cyp11a1*, and the sex-determining gene, *Nr5a1*, were up-regulated specifically in the BPA-treated group. The up-regulation of mRNAs was observed in the mesenchymal component of the UGS as well as in the cerebellum, heart, kidney, and ovary but not in the testis. The number of aromatase-expressing mesenchymal cells in the BPA-treated UGS was approximately twice that in the untreated and DES-treated UGS. The up-regulation of *Esrrg* mRNA was observed in organs for which mRNAs of steroidogenic enzymes were also up-regulated. We demonstrate here that fetal exposure to low-dose BPA has the unique action of increasing in situ E_2 levels and CYP19A1 (aromatase) activity in the mouse UGS. Our data suggest that BPA might interact with in situ steroidogenesis by altering tissue components, such as the accumulation of aromatase-expressing mesenchymal cells, in particular organs.

aromatase, bisphenol A, developmental biology, embryo, estradiol/estrogen receptor, in situ estrogen production, male reproductive tract, prostate, steroidogenic enzyme, urogenital sinus

[1]Supported by Grants-in-Aid from the Ministry of Health, Labor, and Welfare, Japan. GEO accession no. GSE24928.
[2]Correspondence: Yoshiki Sugimura, Department of Nephro-Urologic Surgery and Andrology, Mie University Graduate School of Medicine, 2-174 Edobashi, Tsu, Mie 514-8507, Japan. FAX: 81 59 231 5203; e-mail: sugimura@clin.medic.mie-u.ac.jp
[3]These authors contributed equally to this work.
[4]Current address: Mie University Graduate School of Regional Innovation Studies, 1577 kurimamachiya-cho, Tsu, Mie 514-8507, Japan.

Received: 27 July 2010.
First decision: 19 August 2010.
Accepted: 15 November 2010.

eISSN: 1529-7268 http://www.biolreprod.org
ISSN: 0006-3363

INTRODUCTION

Endocrine-disrupting chemicals (EDCs) have been implicated in the alteration of fetal development of urogenital organs as well as the reproductive and endocrine systems in humans and other species [1]. The fetal development of urogenital organs is induced by endogenous hormonal messages that originate in fetal and maternal hormone systems. Fetal exposure to EDCs disrupts the interactions between endogenous hormones and their receptors, causing adverse effects later in life [2]. In the prostate, both androgens and estrogens play a significant role in development and differentiation as well as in the maintenance of adult homeostasis [3]. Therefore, even small changes in estrogen levels, including those of estrogen-mimicking chemicals, can lead to changes in prostate development and differentiation.

Bisphenol A (BPA), one of the EDCs, is a well-known, ubiquitous, estrogenic chemical used in the manufacture of polycarbonate plastics, as a lining in metal food and drink cans, and in dental sealants [4]. The concern with BPA originates from its detection in maternal and fetal plasma as well as the placenta [5, 6]. Thus, fetal exposure to BPA is implicated in fetal toxicity as well as in subsequent growth of the infant. Histopathologically, fetal exposure to low-dose BPA (10 $\mu g\ kg^{-1}\ day^{-1}$) has been shown to increase cell proliferation of urogenital sinus epithelium (UGE) in the primary prostatic ducts of CD1 mice [7]. Recently, our group reported that fetal exposure to low-dose BPA (20 $\mu g\ kg^{-1}\ day^{-1}$) specifically increased the number of basal epithelial cells in the adult prostate of BALB/c mice and also induced permanent cytokeratin 10 expression in such cells similar to the effects of synthetic estrogen diethylstilbestrol (DES; 0.2 $\mu g\ kg^{-1}\ day^{-1}$) [8]. Epigenetically, neonatal exposure of male rats to low-dose BPA (10 $\mu g\ kg^{-1}\ day^{-1}$) elicited critical molecular changes during prostate development and also increased prostatic gland susceptibility to precancerous neoplastic lesions and hormonal carcinogenesis [9]. Toxicological studies of BPA at less than 50 $\mu g\ kg^{-1}\ day^{-1}$ in rodent fetuses and offspring have demonstrated alterations of mammary gland development, open-field behavior, and reproductive functioning [10–12].

Some EDCs are reported to alter the in situ sex steroid hormonal environment in the reproductive system. The triazine herbicide atrazine binds directly to adrenal-4-binding protein/steroidogenic factor-1 (official symbol NR5A1) and increases CYP19A1 (cytochrome P450 aromatase) expression and, ultimately, estradiol (E_2) production in human genital cancer cell lines [13]. The aryl hydrocarbon (dioxin) also increases CYP19A1 (aromatase) expression mediated by its receptor in mouse ovaries [14]. In contrast, the phosphorothioate insecticide profenofos increases the expression of steroidogenic genes

and testosterone levels in rat testes [15]. Recently reported adverse effects of BPA on in situ steroidogenesis include increased testosterone levels in mouse Leydig cells and decreased E_2 levels in porcine ovarian granulosa cells [16, 17]. Thus, BPA may have the potential not only to mimic estrogenic action but also to alter in situ steroidogenesis in the prostate as well as other reproductive organs.

To investigate the effects of fetal exposure to low-dose BPA on in situ steroidogenesis in the developing prostate, we first measured sex steroid hormone levels and CYP19A1 (aromatase) activity in the BPA-treated mouse urogenital sinus (UGS), from which the prostate develops embryologically. Subsequently, we examined the alterations of steroidogenic enzyme gene expression to confirm the alterations of the in situ sex steroid hormonal environment in the BPA-treated mouse UGS. Finally, we identified the BPA-specific biological effects for in situ steroidogenesis during fetal prostate development.

MATERIALS AND METHODS

Animals

In the present study, 36 pregnant female C57BL/6 mice were purchased on the 12th day of gestation from Japan SLC, where the breeding strategy was to mate three female C57BL/6 mice (age, 10 wk) with one male overnight and separate them the next morning (plug date denoted as Day 0). All animals were housed individually in chip-bedded polyolefin cages in a room with controlled temperature (23 ± 1°C) and humidity (45 to 65%) on a 12L:12D photoperiod. Mice were fed a low-phytoestrogen diet (NIH-07PLD; Oriental Yeast Co.) and tap water ad libitum.

Chemicals

For the present study, both BPA and DES with a purity of 99% or greater were purchased from Nacalai Tesque and Wako Pure Chemical Industries, respectively.

Fetal Exposure to Chemicals

We randomly assigned 36 pregnant female C57BL/6 mice to three different treatment groups: BPA (20 $\mu g\ kg^{-1}\ day^{-1}$, n = 12) or DES (0.2 $\mu g\ kg^{-1}\ day^{-1}$, n = 12), both of which were dissolved in tocopherol-stripped corn oil (MP Biomedical, Inc.), administered by oral gavages on Embryonic Day (E) 13 to E16 and the control group, in which pregnant mice were fed tocopherol-stripped corn oil (2 ml/kg, n = 12). Previously, our group reported that this protocol of fetal exposure to BPA and DES resulted in similar histopathological changes of adult prostate—that is, increased basal epithelial cell number and induction of cytokeratin 10, a classic marker associated with squamous differentiation, in such cells [8]. Our dose level of BPA for the present study was also based on reported results suggesting that BPA is less than 100-fold less potent than DES. The Mie University's Committee on Animal Investigation approved the experimental protocol.

Termination and UGS Dissection

Between E17 and Postnatal Day (P) 1, all animals were terminated by an overdose of isoflurane followed by cervical dislocation. For each of the three groups, from 15 to 18 fetuses (both male and female) from three pregnant mice were collected at E17, E18, P0, and P1. The bladder and urethra were removed and dissected to isolate the UGS, and then the five or six UGS obtained were pooled as one sample. Thus, the 15–18 UGS were divided into three samples at each time point. The UGS, cerebellum, heart, kidney, testis, and ovary were collected in RNAlater (Applied Biosystems).

To isolate pure UGS, other tissues, such as the bladder, urethra, wolffian duct, seminal vesicle, and mullerian duct, were removed from both the male and female urogenital tracts. The histopathology of the mouse UGS was then examined by hematoxylin-and-eosin staining.

Measurements of In Situ E_2 Levels and CYP19A1 (Aromatase) Activity in UGS

The E_2 levels and CYP19A1 (aromatase) activity in UGS were determined by liquid chromatography-tandem mass spectrometry [18] and a tritiated water release assay [19], respectively, which were made available by Aska Pharma Medical. Briefly, the organs were homogenized, and the extracts were applied to a C18 Amprep solid-phase column (Amersham Biosciences) to remove contaminating fats. The E_2 was then separated using a normal-phase high-performance liquid chromatography system (Jasco) with a silica gel column (Cosmosil 5SI; Nacalai Tesque), and 100 pg of isotope-labeled [$^{13}C_4$]E_2 were added to extracts. The evaporated extracts were reacted with 5% pentafluorobenzyl bromide/acetonitrile, under KOH/ethanol, for 1 h at 55°C. After evaporation, the products were reacted with 100 ml of picolinic acid solution (2% picolinic acid, 2% 2-dimethylaminopyridinc, and 1% 2-methyl-6-nitrobenzoic acid in tetrahydrofuran) and 20 ml of triethylamine for 0.5 h at room temperature. The reaction products were dissolved in 1% acetic acid and then purified using a Bond Elute C18 column (Varian). The products were measured with a reverse-phase liquid chromatograph (Agilent 1100; Agilent Technologies) coupled with an API 5000 triple-stage quadrupole mass spectrometer (Applied Biosystems) in the positive-ion mode. This device monitored the *m/z* 558 to *m/z* 339 (E_2) and *m/z* 562 to *m/z* 343 ([$^{13}C_4$]E_2) transitions.

The tritiated water release assay was used for the measurement of CYP19A1 (aromatase) activity. This method measures the production of ^3H_2O, which forms as a result of aromatization of the substrate [1b-^{3}H]androst-4-ene-3,17-dione (New England Nuclear). Serum-free medium containing [1b-^{3}H]androst-4-ene-3,17-dione solution (54 nM) was prepared, of which 0.5 ml was added to each sample. After incubation for 1 h, the samples were placed on ice, and 200 µl of culture medium were withdrawn. The medium was extracted with 500 µl of chloroform, vortexed, and then centrifuged for 1 min at 9000 × *g*. A 100-µl aliquot of the aqueous phase was mixed with 100 µl of a 5% (wt/vol) charcoal/0.5% (wt/vol) dextran T-70 suspension, vortexed, and then incubated at room temperature for 10 min. Then, after centrifugation of the solution for 5 min at 9000 × *g*, a 150-µl aliquot was removed for measurement of radioactivity by liquid scintillation.

RNA Extraction and cDNA Preparation

Total RNA was extracted using the RNeasy Mini Kit (Qiagen, Inc.) in accordance with the manufacturer's instructions. The RNA concentration was then determined spectrophotometrically by a multidetection microplate reader (Dainippon Sumitomo Pharma Co.). From 50 ng of total RNA, cDNA was reverse transcribed using oligo(dT) and Superscript II RNase H-reverse transcriptase (Invitrogen) as previously described [8].

Analysis of Gene Expression Profile

For determining gene expression profiles of the male UGS, GeneChip analysis with the Percellome method was performed [20]. Briefly, organs were prepared using RLT buffer (Qiagen, Inc.). Total RNA was extracted using RNeasy Mini Kit. First-strand cDNA was synthesized by incubating 5 mg of total RNA with a T7 oligo(dT) primer (Invitrogen) according to the manufacturer's protocol. The dsDNA was mixed with T7 RNA polymerase (Enzo Biochem, Inc.). During the in vitro transcription, generated cRNAs were labeled with biotin-16-UTP and biotin-11-CTP (Enzo Biochem, Inc.). The purified cRNA was fragmented at 300–500 bp into the target solution. Hybridization was performed with the GeneChip Mouse Genome 430 Version 2.0 (Affymetrix, Inc.) at 45°C for 18 h after staining with streptavidin-R-phycoerythrin conjugates (Molecular Probes, Invitrogen). The reacted arrays were then scanned as digital image files, and the scanned data were analyzed with GeneChip Operating Software (Affymetrix, Inc.). The expression data were converted to copy numbers of mRNA per cell by the Percellome method, quality controlled, and analyzed using Percellome software [20].

Real-Time PCR Analysis

Real-time PCR was carried out in the iCycler iQ Detection System (Bio-Rad Laboratories) with iQ SYBR-Green Supermix reagents (Bio-Rad Laboratories) as previously described [8]. The PCR amplification reaction was performed with specific primers as shown in Table 1. After PCR, melting-curve analysis was performed to verify specificity and identity of the PCR products. All data were analyzed with the iCycler iQ Optical System Software Version 3.0A (Bio-Rad Laboratories). All PCR data were normalized to *Gapdh* mRNA.

Preparation of Primary Cultured Mesenchymal Cells from UGS

The UGS were dissected from the fetuses and separated into UGE and urogenital sinus mesenchyme (UGM) by tryptic digestion and mechanical separation as previously described [21]. UGM were cultured in RPMI-1640

TABLE 1. Sequences of oligonucleotide primers used for the real-time PCR analyses.

Gene	Primer[a]
Gapdh	F: 5′-AAATGGTGAAGGTCGGTGTG-3′
	R: 5′-TGAAGGGGTCGTTGATGG-3′
Cyp19a1	F: 5′-GCCCAATGAATTTACCCTCGAA-3′
	R: 5′-AAGCCAAAAGGCTGAAAGTACCT-3′
Cyp11a1	F: 5′-TCGACTCCTCAGAACTAAGACCTG-3′
	R: 5′-GTACCCTGGTGTCCTTTATAGCCT-3′
Nr5a1	F: 5′-CCTGGGCTGGCTACCTCTATC-3′
	R: 5′-CGAACTAGAGCCAGAGGAGGAC-3′
Esr1	F: 5′-GCACAGGATGCTAGCCTTGTCTC-3′
	R: 5′-AATTGTCACCAGCTTGCAGGTTC-3′
Ar	F: 5′-GGCGGTCCTTCACTAATGTCAACT-3′
	R: 5′-CTGACTTGTGCATGCGGTACTCAT-3′
Esrrg	F: 5′-CCGAGAGTTGGTGGTTATCATTGG-3′
	R: 5′-GGAAGACCCTCGCCGTGC-3′

[a] F, forward; R, reverse.

with 5% fetal bovine serum and plated out on four-well glass slides (BD Falcon). After several days, cells were fixed in methanol and processed for immunocytochemical analysis.

Immunocytochemical Staining

The sections were first incubated for 15 min in 0.01 M PBS. After inhibition of endogenous peroxidases (10 min in 0.6% H_2O_2 diluted in 0.01 M PBS plus 0.2% Triton X-100 [PBST]) and saturation (2 h in a 5% normal goat serum solution), sections were incubated overnight at 4°C in a polyclonal affinity-purified antiaromatase antibody or estrogen-related receptor gamma (ESRRG) antibody raised in rabbit against quail recombinant aromatase or ESRRG diluted 1:500 in 0.01 M PBST. The next day, the sections were immersed for 2 h at room temperature in a biotin-conjugated goat anti-rabbit immunoglobulin G (DakoCytomation, Inc.) diluted 1:400 in PBST and then for 2 h in a streptavidin-fluorescein complex (Rhodamine; DakoCytomation, Inc.) diluted 1:50 in PBST. Between each step, sections were extensively rinsed in PBST. The sections were mounted onto microscope slides, coverslipped with a gelatin-based mounting medium, and stored in the dark at 4°C. For double-labeling immunofluorescence, Alexa Fluor 488- or 594-conjugated secondary antibodies were used. Rabbit polyclonal anti-aromatase antibody was kindly provided by Prof. Nobuhiro Harada (Department of Biochemistry, Fujita Health University School of Medicine, Aichi, Japan) [22]. The rabbit polyclonal anti-ESRRG antibody used in the present study was established and characterized as previously reported [23]. The mouse monoclonal anti-Ran antibody (Santa Cruz Biotechnology, Inc.) was used to detect nucleus in cells. Ran, also called TC4, is the small RAS-related protein that is localized in the nucleus.

Statistical Analysis

Results are expressed as the mean ± SD. Differences among the three groups were determined using Student *t*-test with Dunnett multiple comparison. A value of $P < 0.05$ was considered to be statistically significant.

RESULTS

BPA-Specific Increases of E_2 Levels and CYP19A1 (Aromatase) Activity in Mouse UGS

The pregnant mice were exposed to low-dose BPA during the onset of prostatic budding (E13–E16), and the UGS of fetuses were collected during bud elongation (E17–P1). In analyses of in situ sex steroid hormonal environment, E_2 levels and CYP19A1 (aromatase) activity were significantly increased only at P1 in BPA-treated UGS, not at P1 in the DES-treated UGS (Fig. 1). At E17 and P1, both the E_2 levels and CYP19A1 (aromatase) activity in untreated male UGS were not significantly different compared with those in untreated female UGS.

BPA-Specific Up-Regulation of Steroidogenic Enzyme and Sex-Determining Gene mRNA in Mouse UGS

To investigate the BPA-specific gene alterations related to increases of the E_2 levels and aromatase activity, we performed preliminary GeneChip analysis with the Percellome method in the BPA- or DES-treated male UGS at E17 and P1. The results showed BPA-specific mRNA up-regulation of steroidogenic enzymes, such as *Cyp11a1*, *Cyp11b1*, and *Cyp17a1*, and sex-determining factors, such as *Nr5a1*, *Nr0b1*, *Gata4*, and *Amhr2* (data not shown). Furthermore, quantitative PCR analysis confirmed the mRNA up-regulation of *Cyp19a1*, *Cyp11a1*, and *Nr5a1* only in the BPA-treated neonatal (P0 and P1) UGS, not in the DES-treated neonatal UGS (Fig. 2). No difference in mRNA expression levels was found between E17 and P1 when comparing the untreated male UGS to that of the female. In

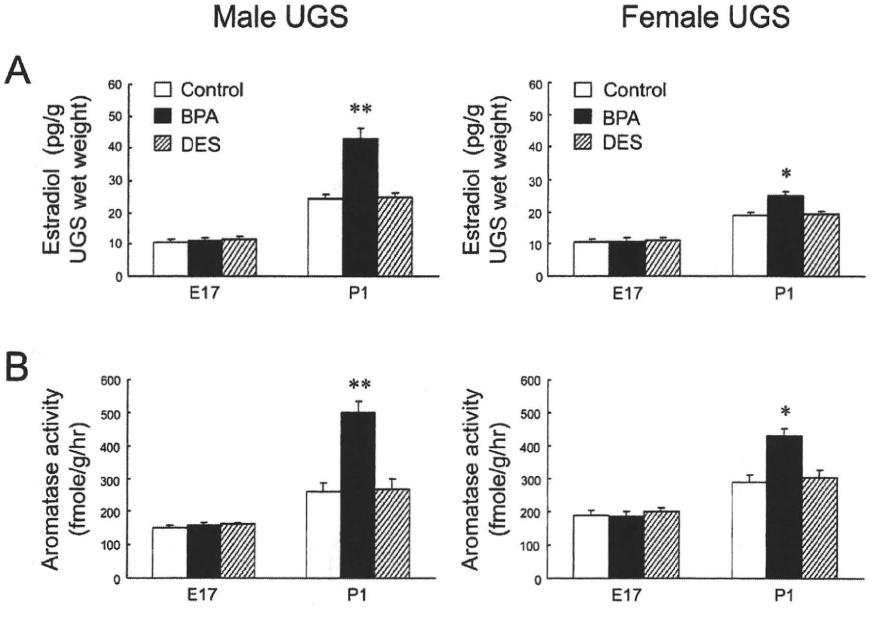

FIG. 1. BPA-specific increases of E_2 levels and CYP19A1 (aromatase) activity in mouse UGS. E_2 levels (**A**) and CYP19A1 (aromatase) activity (**B**) were measured in the untreated control (open bar), BPA-treated UGS (closed bar), and DES-treated UGS (slashed bar) at E17 and P1. *$P < 0.01$, **$P < 0.001$ vs. control.

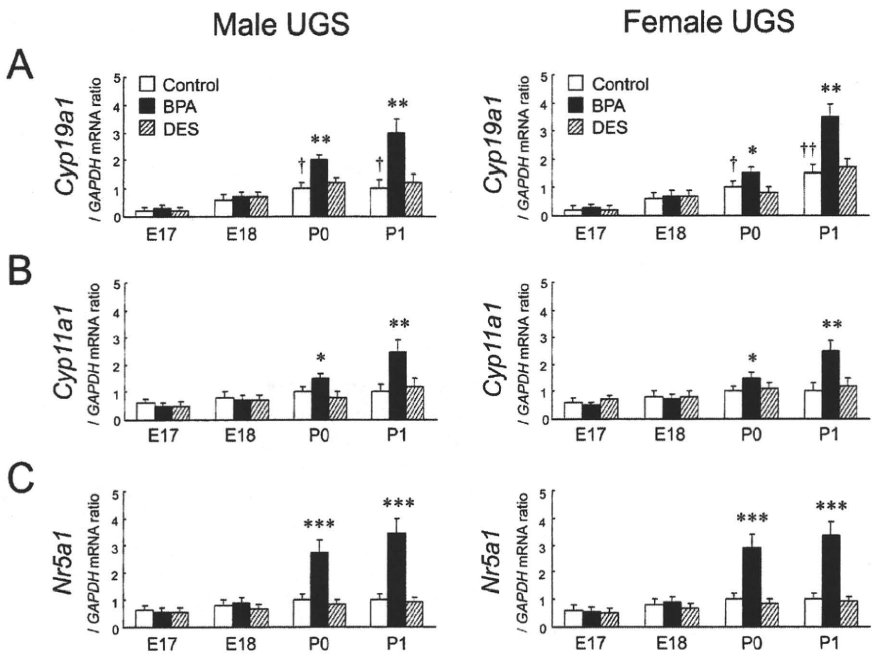

FIG. 2. BPA-specific up-regulation of steroidogenic enzyme and sex-determining gene mRNA in mouse UGS. The relative mRNA expressions of *Cyp19a1* (**A**), *Cyp11a1* (**B**), and *Nr5a1* (**C**) were determined in the untreated control (open bar), BPA-treated UGA (closed bar), and DES-treated UGS (slashed bar) between E17 and P1. $^{*}P < 0.05$, $^{**}P < 0.01$, $^{***}P < 0.001$ vs. control at each time point; $^{\dagger}P < 0.01$, $^{\dagger\dagger}P < 0.001$ vs. control at E17.

untreated male and female UGS, the mRNA of *Cyp19a1* was gradually increased between E17 and P1.

Restricted BPA-Specific Up-Regulation of Steroidogenic Enzyme and Sex-Determining Gene mRNA in UGE and UGM

In male fetuses at P1, it was not feasible to separate UGE and UGM components within the male UGS because of the formation of prostatic buds. In the female at P1, the up-regulation of *Cyp19a1*, *Cyp11a1*, and *Nr5a1* mRNA was observed only in UGM, not in UGE, of the BPA-treated group (Fig. 3). In both male and female UGE, expressions of such mRNAs were quite low and not up-regulated, even in the BPA-treated group. At E17, no difference in mRNA expression levels was found when comparing the untreated male UGM with that of the female.

BPA-Specific Increases of Aromatase-Expressing Cells in Primary Cultured UGM

In both the male and female, P1 UGM was primary cultured in vitro. Representative pictures of aromatase-positive cells are shown in Figure 4, A–C. The aromatase-positive staining was

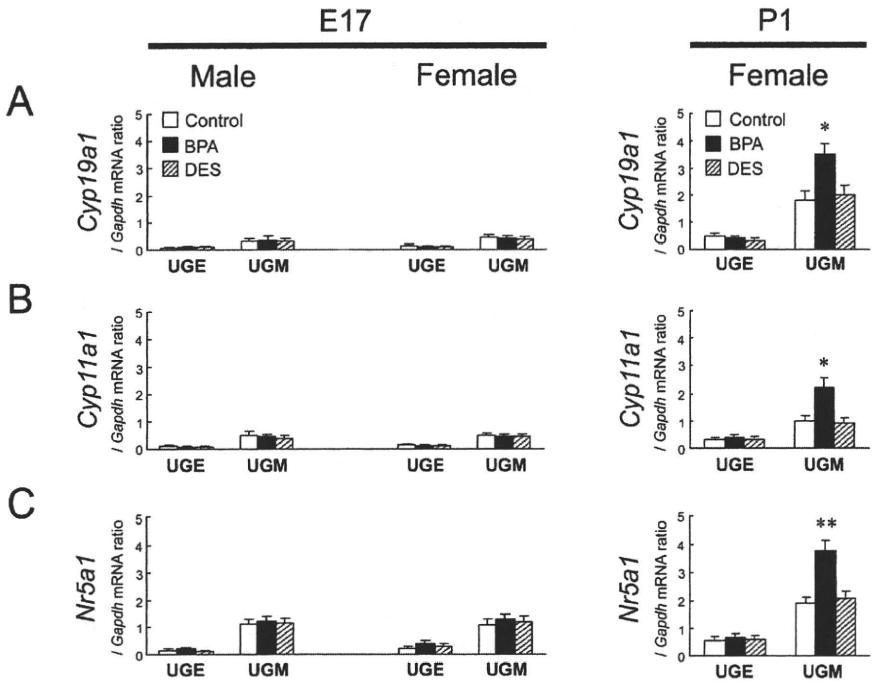

FIG. 3. Restricted BPA-specific up-regulation of steroidogenic enzyme and sex-determining gene mRNA in UGE and UGM. The relative mRNA expressions of *Cyp19a1* (**A**), *Cyp11a1* (**B**), and *Nr5a1* (**C**) were determined for UGE and UGM of the untreated control (open bar), BPA-treated UGS (closed bar), and DES-treated UGS (slashed bar) at E17 and P1. $^{*}P < 0.01$, $^{**}P < 0.001$ vs. control.

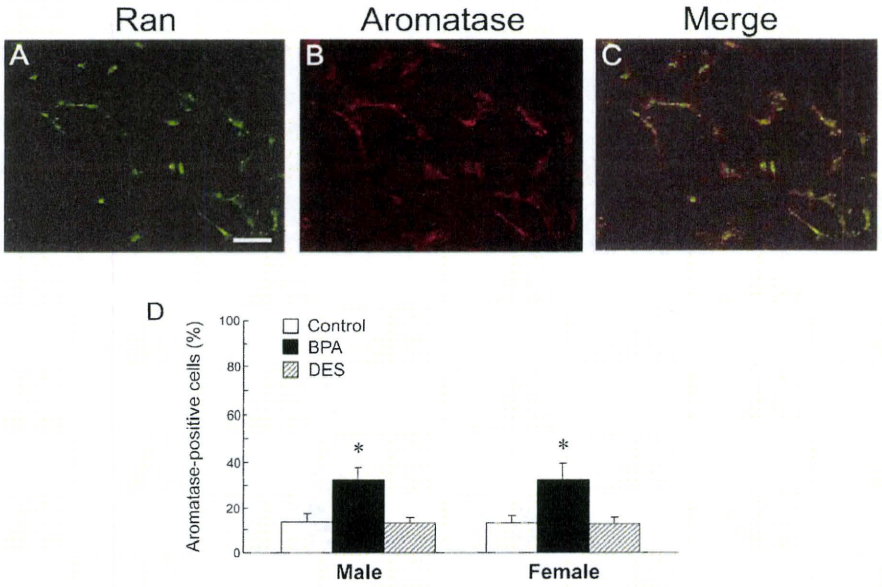

FIG. 4. BPA-specific increases of aromatase-expressing cells in primary cultured UGM. **A**–**C**) Fluorescence signals were detected for the CYP19A1 (aromatase) protein in primary cultured UGM. The nuclei were identified by Ran staining. Bar = 100 μm, magnification ×400. **D**) The number of aromatase-positive cells was counted in primary cultured UGM of the untreated control open bar), BPA-treated UGS (closed bar), and DES-treated UGS (slashed bar), and the percentage of aromatase-positive cells was calculated from at least 10 areas. $*P < 0.01$ vs. control.

observed in the cytoplasm of cultured UGM. The rate of positivity (i.e., the percentage of cells that expressed CYP19A1 [aromatase] protein), was approximately 10% in the untreated and the DES-treated groups, whereas it was as high as approximately 30% in the BPA-treated group (Fig. 4D). No difference in the rate of positivity of CYP19A1 (aromatase) was found when comparing the untreated male UGM to that of the female.

Restricted BPA-Specific Up-Regulation of Esrrg *mRNA in UGE and UGM*

In E17 female UGM, the mRNA expression of *Esr1* was up-regulated by both BPA and DES treatment (Fig. 5A). At E17, however, the mRNA expression of *Ar* was up-regulated by both BPA and DES treatment in the male UGS (Fig. 5B). At P1, mRNA expression of *Ar* was up-regulated by both BPA and DES treatment in the female UGS (Fig. 5B). In both the male and female, the up-regulation of *Esrrg* mRNA was observed at E17 and restricted in UGM, but not in UGE, of the BPA-treated group (Fig. 5C). In both the male and female UGE, the expression of *Esrrg* mRNA was quite low and not up-regulated, even in the BPA-treated group. At E17, no difference in mRNA expression levels was found when comparing the untreated male UGS with that of the female.

BPA-Specific Increases of ESRRG-Expressing Cells in Primary Cultured UGM

In both the male and female, E17 UGM was primary cultured in vitro. Representative pictures of ESRRG-positive

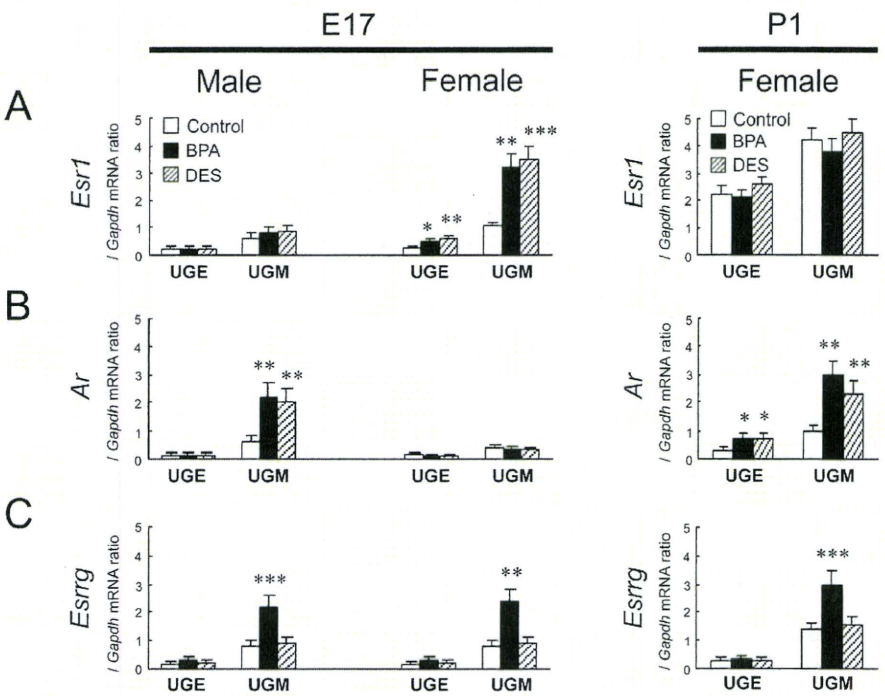

FIG. 5. Restricted BPA-specific up-regulation of *Esrrg* mRNA in UGE and UGM. The relative mRNA expressions of *Esr1* (**A**), *Ar* (**B**), and *Esrrg* (**C**) were determined in UGE and UGM of the untreated control (open bar), BPA-treated UGS (closed bar), and DES-treated UGS (slashed bar) at E17 and P1. $*P < 0.05$, $**P < 0.01$, $***P < 0.001$ vs. control.

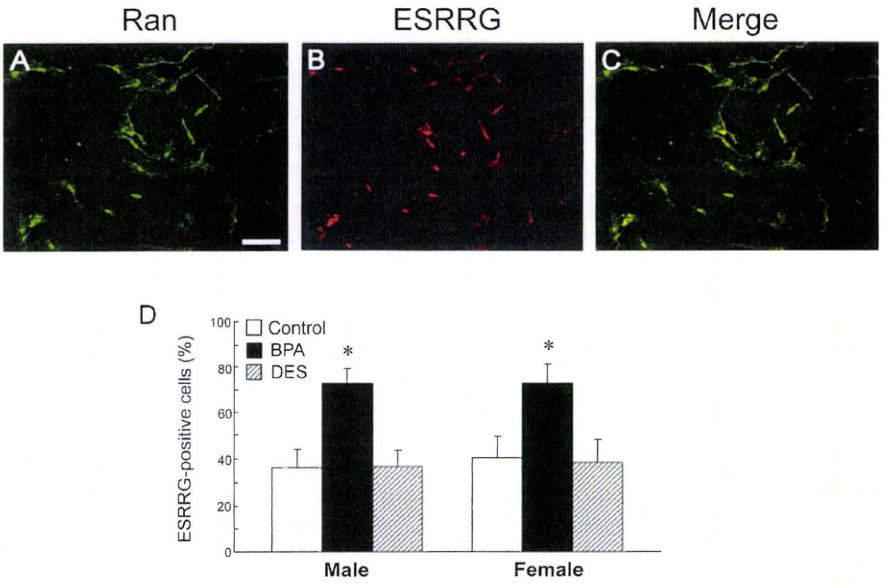

FIG. 6. BPA-specific increases of ESRRG-expressing cells in primary cultured UGM. **A–C**) Fluorescence signals were detected for the ESRRG protein in primary cultured UGM. The nuclei were identified by Ran staining. Bar = 100 μm, magnification ×400. **D**) The number of ESRRG-positive cells was counted in primary cultured UGM of the untreated control (open bar), BPA-treated UGS (closed bar), and DES-treated UGS (slashed bar), and the percentage of ESRRG-positive cells was calculated from at least 10 areas. *$P < 0.01$ vs. control.

cells are shown in Figure 6, A–C. The ESRRG-positive staining was observed in both the nucleus and the cytoplasm of cultured UGM. The number of ESRRG-positive UGM was significantly increased only in the BPA-treated group and showed a 2.2-fold increase in males and a 1.6-fold increase in females (Fig. 6D). No difference was found in the rate of positivity of ESRRG when comparing the untreated male UGM with that of the female.

BPA-Specific Up-Regulation of Esrrg *and Steroidogenic Enzyme mRNA in Sex Hormone-Related Organs*

To investigate the BPA-specific up-regulation of in situ steroidogenesis in other organs, we first examined the changes in *Esrrg* mRNA expression in sex hormone-related organs, such as the cerebellum, heart, kidney, ovary, and testis. At P1, the mRNA expression of *Esr1* in the cerebellum, heart, kidney, and ovary, but not in the testis, was up-regulated by both BPA and DES treatment (Fig. 7A). However, no significant difference in *Ar* mRNA expression was observed in all organs examined (Fig. 7B). In the untreated group, the mRNA expression of *Esrrg* was not detected in the testis at E17 and P1 (Fig. 7C). The up-regulation of *Esrrg* mRNA was observed at E17 and restricted to the cerebellum, heart, kidney, and ovary (Fig. 7C). The BPA-specific up-regulation of *Cyp19a1*, *Cyp11a1*, and *Nr5a1* mRNA was observed only at P1 in the cerebellum, heart, kidney, and ovary, but not in the testis (Fig. 8).

DISCUSSION

Concern about the effects of EDCs such as BPA on human health has been increasing [24]. Although the majority of EDCs have the potential to alter functioning of the reproductive and endocrine system, the actual mechanism responsible for such alterations has not been identified thoroughly. BPA is of concern because its chemical structure resembles that of DES. Several studies have reported that BPA can mimic estrogen action, such as induction of vaginal cornification, uterine vascular permeability, growth and differentiation of the mammary gland, and synaptic plasticity in the hippocampus [25–28]. In the prostate, alterations in normal development can produce permanent changes that persist throughout adulthood and may increase the risk of disease in later life [9]. Thus, our objective was to investigate the biological effects of low-dose BPA on the initial development of primary ducts in the fetal prostate.

During prostatic development, alteration of sex steroid hormone synthesis may be responsible for prostatic anomalies associated with fetal exposure to EDCs. In the present study, fetal exposure to low-dose BPA increased E_2 levels in P1 UGS of both the male and female, whereas DES-induced changes were not detected. This alteration was also correlated with increased activity of CYP19A1 (aromatase) in UGS at P1, suggesting the unique action of BPA for in situ steroidogenesis in UGS. The BPA-specific increase of E_2 levels in UGS at P1 was correlated with the following: mRNA up-regulation of steroidogenic enzymes, such as *Cyp19a1* and *Cyp11a1*, and an increased number of aromatase-expressing UGM. The enzyme CYP19A1 (aromatase) is responsible for in situ E_2 production and the crucial testosterone/E_2 balance necessary for normal embryonic and fetal development, even in males. The data presented here shows that the up-regulation of *Cyp19a1* mRNA in BPA-treated UGM was comparable to changes in both in situ E_2 production and CYP19A1 (aromatase) activity.

In the present study, we demonstrated that the BPA-specific increase in steroidogenic enzyme mRNA and aromatase-expressing cell number were observed in both the male and female UGM. During embryonic development, the mesenchymal component is involved in the induction and organogenesis of various organs, including the prostate, mammary gland, lung, kidney, and pancreas. It has been well established that subpopulations of the mesenchymal component are a source of potent molecules that regulate epithelial growth and differentiation [29]. In the prostate, androgen-responsive signals derived from UGM permissively and instructively induce UGE to form primary ducts of the prostate [30].

Comparison between the neonatal male and female UGS shows a similarity in the condensed mesenchyme of the ventral areas—that is, the ventral prostate mesenchyme (VPM) in the male and the ventral mesenchymal pad (VMP) in the female [31]. In the male, a defined VPM is specifically associated with ductal branching morphogenesis and cytodifferentiation of the ventral prostate. Females do not usually form a prostate. In a

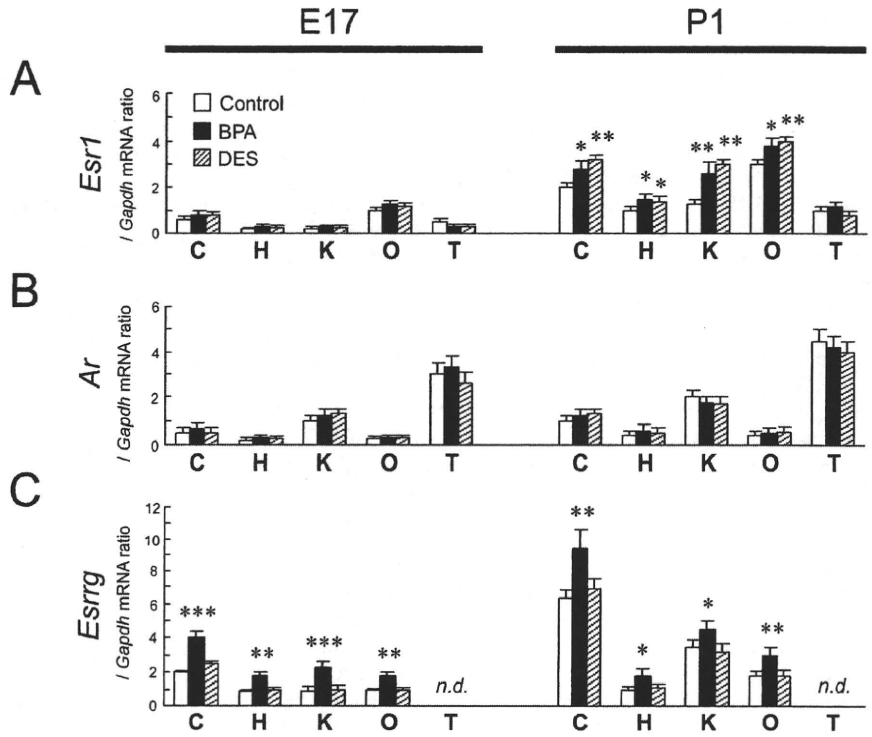

FIG. 7. BPA-specific up-regulation of *Esrrg* mRNA in sex steroid hormone-related organs. The relative mRNA expressions of *Esr1* (**A**), *Ar* (**B**), and *Esrrg* (**C**) were determined in sex steroid hormone-related organs of the untreated control (open bar), BPA-treated UGS (closed bar), and DES-treated UGS (slashed bar) at E17 and P1. C, cerebellum; H, heart; K, kidney; O, ovary; T, testis; *n.d.*, not detected. $^{*}P < 0.05$, $^{**}P < 0.01$, $^{***}P < 0.001$ vs. control.

tissue recombination model, the female VMP induces prostate development in response to androgens [32], suggesting that cells within the female VMP have prostatic-inductive activity. Moreover, an earlier tissue recombination study showed that the ability of the female UGS to respond to androgens in forming prostate was gradually lost between P1 and P5 [33]. These results suggest strongly that androgen-responsive regulatory molecules are expressed constitutively even in the female VMP. Although the female VMP forms in the absence of androgens, androgen receptor (AR) expression was observed in the neonatal female VMP in a pattern similar to that observed in the male VPM [34]. Therefore, the BPA-specific increase in E_2 levels might interact with the intracellular AR signaling in both the male VPM and the female VMP. However, to our knowledge,

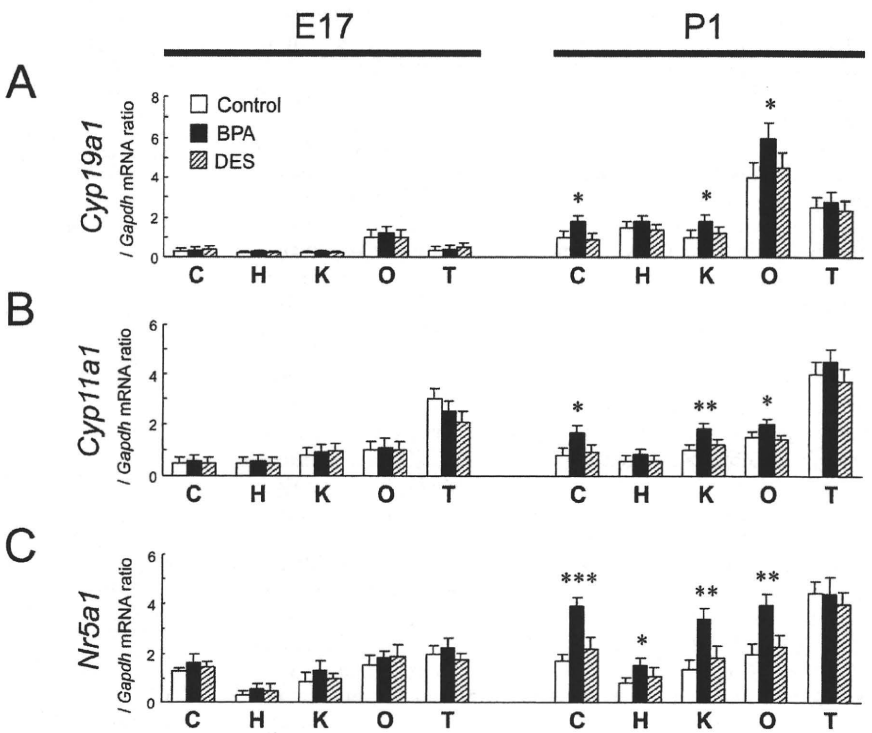

FIG. 8. BPA-specific up-regulation of steroidogenic enzyme and sex-determining gene mRNA in sex steroid hormone-related organs. The relative mRNA expressions of *Cyp19a1* (**A**), *Cyp11a1* (**B**), and *Nr5a1* (**C**) were determined in sex steroid hormone-related organs of the untreated control (open bar), BPA-treated UGS (closed bar), and DES-treated UGS (slashed bar) at E17 and P1. C, cerebellum; H, heart; K, kidney; O, ovary; T, testis. $^{*}P < 0.05$, $^{**}P < 0.01$, $^{***}P < 0.001$ vs. control.

the morphological changes in neonatal female UGS have not yet been investigated.

Our results suggest that BPA has a stimulatory effect on in situ steroidogenesis in P1 UGS of both the male and female at low-dose exposure levels. Recently, ESRRG has been reported to bind strongly with BPA [35]. Susens et al. [36] have reported that expression of ESRRG in the mouse is organ-specific: ESRRG is expressed in the brain, heart, kidney, and skeletal muscle but not in the lung, spleen, and testis. In the present study, the up-regulation of *Cyp19a1* and *Cyp11a1* mRNA by BPA treatment was detected only in organs expressing *Esrrg* mRNA. These data suggest that the possibility of a stimulatory effect on in situ steroidogenesis by fetal exposure to low-dose BPA may be a concern not only in UGS but also in organs expressing ESRRG, such as the brain, heart, kidney, and ovary. It is important to note that Takeda et al. [23] have recently reported that ESRRG was detected in the human testis, suggesting that the distribution of ESRRG differs slightly between mice and humans.

In the present study, the BPA-specific up-regulation of steroidogenic enzyme mRNA in UGS, cerebellum, heart, kidney, and ovary was observed only during the neonatal period (i.e., P0 and P1) and not during the prenatal period (i.e., E17 and E18). During pregnancy in rodents, large amounts of estrogens produced in the maternal ovaries are continuously delivered to the fetus through the placenta. After birth, however, the fetus may be released from the maternal, high-estrogen environment. Thus, one possibility is that the maternal, high-estrogen environment in pregnancy may protect the fetus from the effect of BPA on in situ steroidogenesis during the prenatal period. However, we did not investigate the effects of neonatal BPA treatment on in situ steroidogenesis.

The EDC-induced alterations of the in situ estrogen environment depend on each compound. In addition to atrazine and dioxin, the organotin compound tributyltin also increases E_2 production in human placental choriocarcinoma cells [37]. Tributyltin has been demonstrated to induce the superimposition of male sex organs, such as a penis and/or a vas deferens, over female sex organs, which is a phenomenon known as imposex [38]. These studies suggest strongly that EDCs might affect fetal development not only by mimicking the actions of sex steroid hormones but also by alteration of in situ steroidogenesis.

In the prostate, AR expressed in mesenchyme is required for directing growth and branching morphogenesis of epithelia, presumably by induction of growth factors [39]. In the present study, fetal exposure to BPA or DES increased *Ar* mRNA expression in E17 UGM of the male, whereas *Esr1* mRNA expression was up-regulated in E17 UGM of the female. Recently, Richter et al. [40] have reported that in vitro BPA treatment stimulates *Ar* and *Esr1* mRNA expression in mesenchymal cells isolated from fetal mouse prostate. Thus, our results support the idea that BPA-induced cell proliferation of the primary prostatic ducts may be caused by inducing *Ar* mRNA expression in the male UGM. In contrast, the induction of *Esr1* mRNA expression by BPA or DES may create a positive-feedback loop in the female UGM. Further investigation and morphological analysis will be necessary to confirm the effects of up-regulated ESR1 in the female UGS.

In conclusion, we have shown the unique action of BPA in the mouse UGS. Specifically, we have demonstrated that the increases in E_2 levels and CYP19A1 (aromatase) activity were observed in the BPA-treated UGS but not in the DES-treated UGS. Ricke et al. [41] have recently reported that stromal hormone imbalance, a potential source of local E_2 production, may be responsible for prostatic disease, such as benign prostatic hyperplasia and prostate cancer. The data in the present study give rise to the concept that the development and differentiation of UGS in mouse fetuses is very sensitive to fetal exposure to low-dose BPA via the mother. Further investigation of various aspects of BPA-specific action is necessary to fully understand the role of BPA as an EDC.

ACKNOWLEDGMENTS

We thank Prof. Nobuhiro Harada at Department of Biochemistry, Fujita Health University School of Medicine, Aichi, Japan, for kindly providing rabbit polyclonal antiaromatase antibody. We also thank Mrs. Hiroko Nishii for technical support.

REFERENCES

1. Sekizawa J. Low-dose effects of bisphenol A: a serious threat to human health? J Toxicol Sci 2008; 33:389–403.
2. Newbold RR, Jefferson WN, Padilla-Banks E. Prenatal exposure to bisphenol A at environmentally relevant doses adversely affects the murine female reproductive tract later in life. Environ Health Perspect 2009; 117:879–885.
3. McPherson SJ, Ellem SJ, Risbridger GP. Estrogen-regulated development and differentiation of the prostate. Differentiation 2008; 76:660–670.
4. Welshons WV, Nagel SC, vom Saal FS. Large effects from small exposures. III. Endocrine mechanisms mediating effects of bisphenol A at levels of human exposure. Endocrinology 2006; 147:S56–S69.
5. Schonfelder G, Wittfoht W, Hopp H, Talsness CE, Paul M, Chahoud I. Parent bisphenol A accumulation in the human maternal-fetal-placental unit. Environ Health Perspect 2002; 110:A703–A707.
6. Tsutsumi O. Assessment of human contamination of estrogenic endocrine-disrupting chemicals and their risk for human reproduction. J Steroid Biochem Mol Biol 2005; 93:325–330.
7. Timms BG, Howdeshell KL, Barton L, Bradley S, Richter CA, vom Saal FS. Estrogenic chemicals in plastic and oral contraceptives disrupt development of the fetal mouse prostate and urethra. Proc Natl Acad Sci U S A 2005; 102:7014–7019.
8. Ogura Y, Ishii K, Kanda H, Kanai M, Arima K, Wang Y, Sugimura Y. Bisphenol A induces permanent squamous change in mouse prostatic epithelium. Differentiation 2007; 75:745–756.
9. Ho SM, Tang WY, Belmonte de Frausto J, Prins GS. Developmental exposure to estradiol and bisphenol A increases susceptibility to prostate carcinogenesis and epigenetically regulates phosphodiesterase type 4 variant 4. Cancer Res 2006; 66:5624–5632.
10. Markey CM, Luque EH, Munoz de Toro M, Sonnenschein C, Soto AM. In utero exposure to bisphenol A alters the development and tissue organization of the mouse mammary gland. Biol Reprod 2001; 65: 1215–1223.
11. Honma S, Suzuki A, Buchanan DL, Katsu Y, Watanabe H, Iguchi T. Low-dose effect of in utero exposure to bisphenol A and diethylstilbestrol on female mouse reproduction. Reprod Toxicol 2002; 16:117–122.
12. Kubo K, Arai O, Omura M, Watanabe R, Ogata R, Aou S. Low-dose effects of bisphenol A on sexual differentiation of the brain and behavior in rats. Neurosci Res 2003; 45:345–356.
13. Fan W, Yanase T, Morinaga H, Gondo S, Okabe T, Nomura M, Komatsu T, Morohashi K, Hayes TB, Takayanagi R, Nawata H. Atrazine-induced aromatase expression is SF-1 dependent: implications for endocrine disruption in wildlife and reproductive cancers in humans. Environ Health Perspect 2007; 115:720–727.
14. Baba T, Mimura J, Nakamura N, Harada N, Yamamoto M, Morohashi K, Fujii-Kuriyama Y. Intrinsic function of the aryl hydrocarbon (dioxin) receptor as a key factor in female reproduction. Mol Cell Biol 2005; 25: 10040–10051.
15. Moustafa GG, Ibrahim ZS, Hashimoto Y, Alkelch AM, Sakamoto KQ, Ishizuka M, Fujita S. Testicular toxicity of profenofos in matured male rats. Arch Toxicol 2007; 81:875–881.
16. Song KH, Lee K, Choi HS. Endocrine disrupter bisphenol A induces orphan nuclear receptor Nur77 gene expression and steroidogenesis in mouse testicular Leydig cells. Endocrinology 2002; 143:2208–2215.
17. Mlynarcikova A, Kolena J, Fickova M, Scsukova S. Alterations in steroid hormone production by porcine ovarian granulosa cells caused by bisphenol A and bisphenol A dimethacrylate. Mol Cell Endocrinol 2005; 244:57–62.
18. Hojo Y, Higo S, Ishii H, Ooishi Y, Mukai H, Murakami G, Kominami T, Kimoto T, Honma S, Poirier D, Kawato S. Comparison between